# Delft University of Technology

## Three-Phase Medium-Voltage Medium-Frequency Transformer for SST in Green Hydrogen Production

Mirzadarani, Reza; Ghaffarian Niasar, Mohamad; Li, Zhengzhao; Qin, Zian; Vaessen, Peter; Bauer, Pavol; Van Lieshout, Lou

**Citation (APA)**
Mirzadarani, R., Ghaffarian Niasar, M., Li, Z., Qin, Z., Vaessen, P., Bauer, P., & Van Lieshout, L. (2023). Three-Phase Medium-Voltage Medium-Frequency Transformer for SST in Green Hydrogen Production. In *Proceedings of the IECON 2023- 49th Annual Conference of the IEEE Industrial Electronics Society* (Proceedings of the Annual Conference of the IEEE Industrial Electronics Society). IEEE. https://doi.org/10.1109/IECON51785.2023.10312546

**Important note**
To cite this publication, please use the final published version (if applicable).
Please check the document version above.

# Three-Phase Medium-Voltage Medium-Frequency Transformer for SST in Green Hydrogen Production

Reza Mirzadarani
*dept. Electrical Sustainable Energy*
*Delft University of Technology*
Delft, Netherlands
R.Mirzadarani@tudelft.nl

Mohamad Ghaffarian Niasar
*dept. Electrical Sustainable Energy*
*Delft University of Technology*
Delft, Netherlands
M.GhaffarianNiasar@tudelft.nl

Zhengzhao Li
*dept. Electrical Sustainable Energy*
*Delft University of Technology*
Delft, Netherlands
Z.Li-20@tudelft.nl

Zian Qin
*dept. Electrical Sustainable Energy*
*Delft University of Technology*
Delft, Netherlands
Z.Qin-2@tudelft.nl

Peter Vaessen
*dept. Electrical Sustainable Energy*
*Delft University of Technology*
Delft, Netherlands
P.T.M.Vaessen@tudelft.nl

Pavol Bauer
*dept. Electrical Sustainable Energy*
*Delft University of Technology*
Delft, Netherlands
P.Bauer@tudelft.nl

Lou Van Lieshout
*VONK*
Zwolle, Netherlands
lou.vanlieshout@iivonk.com

*Abstract*— **Green hydrogen production uses renewable energies to energise the electrolysers for hydrogen production. The present paper compares possible solutions and configurations of a medium-frequency transformer (MFT) as part of a solid-state transformer (SST) in green hydrogen production applications. The single-phase and three-phase MFTs are compared and it is shown that a Yd three-phase MFT is the optimum choice for applications that require high power delivery and step-down of the voltage. A summary of previous works about MFT is also provided. Three-phase SST based on modular multi-level converters (MMC) is then described and various cases are investigated to obtain the optimum operational frequency. A 25 MVA, 400 Hz, 25.4 kV / 560V oil-immersed MFT design is presented and is shown that the proposed 400 Hz transformer saves 69% of the active parts' weight compared to a conventional line-frequency transformer (LFT).**

*Keywords—electrolyzer, solid-state transformer, medium-frequency transformer*

## I. INTRODUCTION

Green hydrogen production is considered a solution to modern world challenges like climate change and global warming. Hydrogen is an energy source for fuel cells, and there is a rising trend of hydrogen use in vehicles. Furthermore, several industries such as refining petroleum, treating metals, producing fertilizer, and processing foods, use hydrogen for their production. Green hydrogen production uses renewable energies to energise the electrolysers for hydrogen production. While renewable energies are vastly available, a main challenge is to effectively harness and transport the energy produced from these resources. Off-shore wind farms are considered green and reliable energy sources for green hydrogen production [1]. In case of a long distance between these off-shore wind farms and the hydrogen production facilities, HVDC submarine cables are used to transmit generated power to the shore and utilizing a MMC, DC is converted to AC and is then stepped down using a transformer to feed the medium-voltage AC grid to energize the electrolyzer (Fig. 1). Traditionally, 6, 12, or 24 pulse rectifiers can be used to convert the AC input to the required DC for electrolyzer as shown in Fig. 1 (a). The main aim of higher-order rectifiers (12 or 24-pulse rectifiers) is to reduce THD. However, it is possible to reduce the weight and size of the power conversion stage using solid-state transformers (SSTs). The main idea of an SST is to increase the frequency to increase the power density. As shown in Fig. 1 (b), a typical SST for green hydrogen production is made of four main parts: 1) input rectifier, 2) inverter, 3) medium-frequency transformer, and 4) output rectifier.

SSTs operate at higher frequencies; consequently, they have higher power density. They can control the power flow and provide protection. Furthermore, SSTs have several other advantages, such as reduced size and weight compared to line-frequency transformers (LFTs), instantaneous voltage regulation, fault isolation, power factor correction, control of active and reactive power flow, fault current management on low-voltage and high-voltage side. While with the current state-of-the-art power electronics technology, MW range SSTs are more complicated and expensive than LFTs; however, the aforementioned additional values offered by SST as well as reduction in cost and advancement in PE technology can justify their usage in the future grid.

There are several challenges regarding higher operating frequency of an SST. Skin effect and proximity effect result in extra losses in windings. Non-sinusoidal flux, eddy current, and higher hysteresis loss give rise to extra core losses. In addition, SST connected to the grid needs a medium-voltage insulation system which is known to be more complex at higher frequencies due to faster insulation aging. Furthermore, there are challenges in the power electronics parts, like dealing with switching loss or device selections.

While various IGBTs and SiC MOSFETs are available in the market, proper selection of switches depends on the application and structure of the SST. IGBTs are a better choice for lower frequencies and higher powers, whereas according to recent technology developments, SiC MOSFETs are popular for higher frequency range; however, their power rating is limited compared to the IGBTs. To deal with some of the difficulties in SSTs such as limited ratings of the switching devices, using modular multilevel converters (MMCs) is being considered . The main idea of an MMC is to employ a number of cascade full-bridge (or half-bridge) modules to deal with the high-voltage requirement [2]. MMCs can convert AC to DC or vice versa. The output of the MMC can be single-phase or
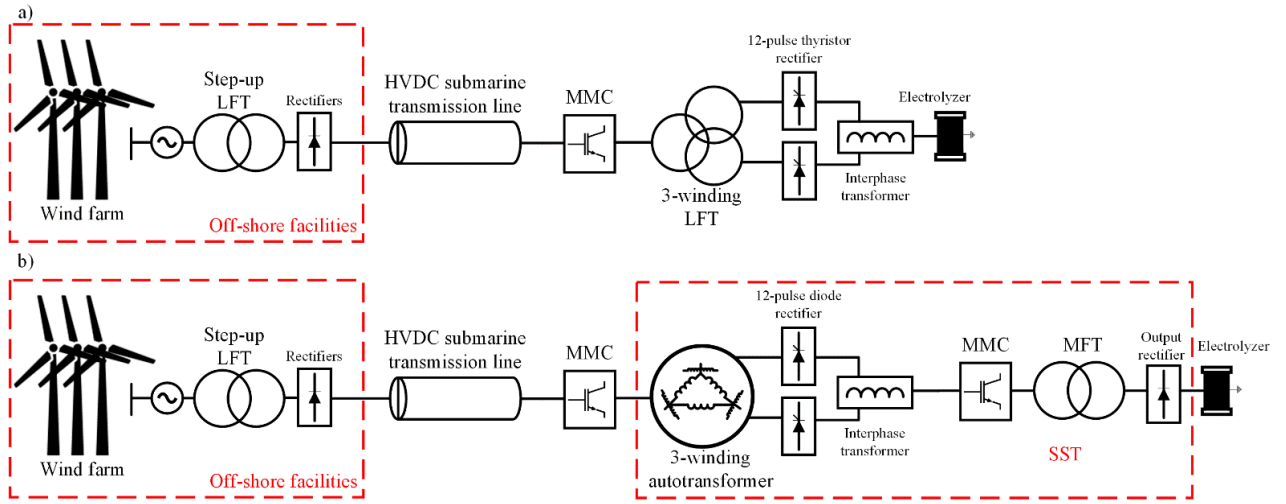
Fig. 1. Green hydrogen production; a) using conventional LFT and rectifier, b)using solid-state transformer (SST)

three-phase [2]. Regarding Fig. 1 (b), the selected structure for the SST is to employ a diode-bridge rectifier (DRU) connected to a DC/AC MMC (as the inverter of the DC/DC converter). It is noteworthy that SST can be single-phase or three-phase.

The central part of SST is the medium-frequency transformer (MFT). The MFT converts the voltage level and also provides galvanic isolation. Therefore, the optimal design of the MFT has a considerable impact on the final weight and size of the SST. Core shape of MFTs can be divided into categories: core-type and shell-type (Fig. 2). There are other possible structures, such as matrix-type MFTs [1]; however, they are not popular in the literature. Each type has its advantages and drawbacks. When lower leakage inductance is needed, shell-type MFTs are the better choice; moreover, they provide better heat dissipation for the core [3]. Nevertheless, in some cases (i.e. MFTs, which are connected to resonant converters), the reduction of leakage inductance is not a preference. In this case, the leakage inductance of the transformer can be considered as the series inductance (or at least a part of the required series inductance). Accordingly, core-type MFTs offers more advantages for these applications.

MFTs can be divided into two other categories: single-phase and three-phase. Using three-phase MFT results in a three-phase SST, which has advantages and disadvantages. Generally speaking, for high-power applications, using three-phase SST has advantages due to the fact that three-phase converter requires a lower transformer rating, and the DC bus capacitors should provide relatively less RMS current. Nonetheless, the number of switches is higher, and the control is more complicated in a three-phase SST.

The concept of a SST is not new; hence, numerous studies have been carried out on this topic. Table I summarizes the features of 29 studies in this field. The comparison items are power level, frequency, core materials, insulation, cooling method, winding, and structure. Only one of them is three-phase. From the core material point of view, 13 out of 29 used Nanocrystalline cores, 10 out of 29 employed ferrite cores, and the rest used silicon steel or amorphous. From the core structure point of view, the majority of previous works used shell-type transformers (16 out of 29). Others employed core type and matrix type. For 5 of them, the structure is not reported. In summary, a shell-type Nanocrystalline/Amorphous transformer with Litz wire windings is the most common solution.
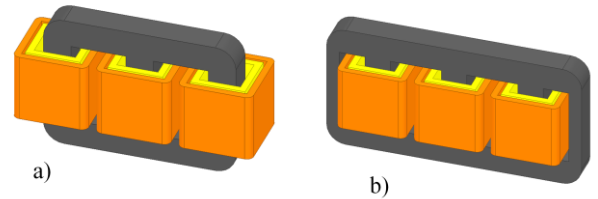


Fig. 2. Transformer types; a) core-type, b) shell-type

The present paper is organized as follows. Section II compares three-phase and single-phase MFTs to illustrate why using three-phase medium-frequency transformers is beneficial in applications such as green hydrogen production that require a considerable current for the load. Section III discusses the optimum frequency selection. A summary of the designed 25 MVA MFT is described in section IV. Finally, section V concludes the paper.

## II. THREE-PHASE MFT

In most of the literature, single-phase SSTs are studied and introduced. The main reason for the popularity of single-phase transformers in the literature is the fact that the rating power of most of the previous works is limited to a few kVA. However, a real SST for green hydrogen production must deliver tens of MVA. Accordingly, using a three-phase SST is beneficial, as shown in the following section. The schematic of a three-phase SST is shown in Fig. 3.

Choosing between single-phase and three-phase SSTs depends on the power electronics and transformer section; nevertheless, Table II compares them regarding the MFT. Furthermore, the comparison between three-phase and single-phase transformers depends on the application and configuration of the MFT. Since the present study focuses on a step-down transformer required for green hydrogen production, the selected configuration is Yd (primary-star-secondary-delta) for two reasons. Firstly, in a star winding, the effective voltage of each phase is calculated as

$$V_{Phase} = \frac{V_{L-L}}{\sqrt{3}} \qquad (1)$$

Where $V_{L-L}$ is the line-to-line voltage. Therefore, a lower voltage is connected to the primary winding. Secondly, in a delta winding, the line current is calculated as follows:

$$I_{Line} = \sqrt{3} \times I_{Phase} \qquad (2)$$

TABLE I. THE COMPARISON OF THE PREVIOUS WORKS

| No | Title | Power (kVA) | Freq. (kHz) | Core Material | Insulation | Cooling Method | Winding | Structure |
|----|-------|-------------|-------------|---------------|------------|----------------|---------|-----------|
| 1 | ABB, 2002 [7] | 350 | 10 | Nanocrystalline | Solid | Water | Coaxial | Shell |
| 2 | ALSTOM, 2003 [8] | 1500 | 5 | Ferrite | Oil | Oil | Litz | NA |
| 3 | TU Delft, 2005 [9] | 50 | 25 | Nanocrystalline | NA | Water | Foil | Shell |
| 4 | ABB PETT, 2007 [34] | 75 | 0.4 | SiFe | Oil | Oil | Wire | NA |
| 5 | Bombardier, 2007 [10] | 350 | 8 | Nanocrystalline | Solid | Water | Hollow | Shell |
| 6 | West Bohemia, 2008 [11] | 12 | 0.4 | NA | Solid | Air | NA | NA |
| 7 | KTH, 2009 [12] | 3000 | 0.5 | Amorphous | Solid | Air | Litz | Shell |
| 8 | KTH, 2009 [13] | 170 | 4 | Amorphous | NA | Water + Oil | Litz + Foil | Shell |
| 9 | FAU-EN, 2011 [14] | 450 | 5.6 | Nanocrystalline | NOMEX + Oil | Water + Oil | Hollow (Al) | Core |
| 10 | IKERLAN, 2012 [15] | 400 | 5 | Nanocrystalline and SiFe | NA | Air | NA | Shell + Core |
| 11 | FREEDM, Gen. I [28] | 20 | 3 | Amorphous | Solid | Air | NA | Core |
| 12 | FREEDM, Gen. II [16] | 20 | 10 | Amorphous | Solid | Air | NA | Core |
| 13 | FREEDM, Gen. III [17] | 20 | 40 | NA | Solid | Air | NA | NA |
| 14 | ABB, 2013 [29] | 150 | 1.75 | Nanocrystalline | Oil | Oil | Wire | Shell |
| 15 | ETH, 2014 [18] | 166 | 20 | Nanocrystalline and Ferrite | Solid | Water and air | Litz | Shell |
| 16 | STS, 2014 [19] | 450 | 8 | Nanocrystalline | Oil + Solid | Air + Oil | Litz | Core |
| 17 | Chalmers, 2016 [30] | 50 | 5 | Nanocrystalline and Ferrite | NA | Air | Litz | Shell |
| 18 | Osaka, 2017 [31] | 5 | 0.4 to 3 | Nanocrystalline and Amorphous | Solid | Air | NA | NA |
| 19 | ETH, 2017 [20] | 144 | 100 | Ferrite | Oil + Solid | Oil | Litz | Shell |
| 20 | ABB, 2017 [32] | 240 | 10 | Nanocrystalline | Solid | Air | Litz | Shell |
| 21 | EPFL, 2017 [21] | 100 | 10 | Ferrite | Air | Air | Litz | Shell |
| 22 | Virginia Tech, 2018 [22] | 15 | 500 | Ferrite | Solid | Air | Litz | Core |
| 23 | NEDO, 2018 [23] | 500 | 3 | Amorphous | Solid | Air | Foil | Core |
| 24 | ETH, 2019 [24] | 25 | 48 | Ferrite | Solid | Air | Litz | Shell |
| 25 | XJTU, 2019 [33] | 10 | 10 | Ferrite | Solid | Air | Litz | Shell |
| 26 | Chalmers, 2020 [1] | 50 | 5 | Ferrite | Oil | Oil | Litz | Matrix |
| 27 | Wisconsin, 2020 [25] | 25 | 50 | Ferrite | Solid | Air | Litz | Shell |
| 28 | Texas, 2020 [26] | 200 | 15 | Nanocrystalline | Solid | Air | Litz | Shell |
| 29 | Tsinghua, 2021 [27] | 60 | 10 | Nanocrystalline | Solid | Conduction | Litz | Core |

Where $I_{Phase}$ is the phase current. Thus, the secondary winding deals with a lower current level. The cross-section area of the magnetic core is calculated as follows

$$A_c = \frac{V_p}{k_w \times k_c \times B_m \times N_p \times f} \quad (3)$$

Where $B_m$ is the maximum magnetic flux density, $N_p$ is the number of primary turns, and $f$ is the frequency. $k_w$ and $k_c$ are the waveform and core stacking factors, respectively. According to (1) and Table II, for the single-phase case $V_{p1} = 2 \times V_{p3}$. Considering $N_{p1} = N_{p3}$ and all other parameters the same results in

$$A_{c1} = 2 \times A_{c3} \quad (4)$$

Where $A_{c1}$ and $A_{c3}$ are the cross-section area of single-phase and three-phase cores, respectively. The rating power of a single-phase transformer is calculated by

$$S_1 = I_{p1} \times V_{p1} \quad (5)$$

Where $I_{p1}$ is the primary current of the single-phase case and $V_{p1}$ is the primary voltage of the single-phase case. The rating power for a three-phase transformer is calculated by

$$S_3 = 3 \times I_{p3} \times V_{p3} \quad (6)$$

Where $I_{p3}$ is the primary current of the three-phase case. In order to make the comparison, let $S_1 = S_3 = S$.

The area product of a single-phase transformer is calculated as follows

$$AP_1 = A_{w1} \times A_{c1} \quad (7)$$

However, the area product for a three-phase transformer is defined differently as follows [4]

$$AP_3 = \frac{3}{2} A_{w3} \times A_{c3} \quad (8)$$

Regarding Table II, the area product of single-phase and three-phase transformers can be compared as

$$AP_1 = AP_3 \quad (9)$$

TABLE II. SINGLE-PHASE VS THREE-PHASE TRANSFORMERS

| Parameter | Single-phase | Three-phase |
|-----------|--------------|-------------|
| Primary voltage ($V_{p,rms}$) | $\frac{\sqrt{2}}{2} \times V_{DC}$ | $\frac{\sqrt{2}}{4} \times V_{DC}$ |
| Core cross-section area ($A_c$) | $\frac{\frac{\sqrt{2}}{2} \times V_{DC}}{k_c k_w B_m N_{p1} f}$ | $\frac{\frac{\sqrt{2}}{4} \times V_{DC}}{k_c k_w B_m N_{p3} f}$ |
| Primary current ($I_p$) | $\sqrt{2} \times \frac{S}{V_{DC}}$ | $\frac{2\sqrt{2}}{3} \times \frac{S}{V_{DC}}$ |
| Primary area ($A_p$) | $\frac{\sqrt{2} N_{p1} S}{J \times V_{DC}}$ | $\frac{2\sqrt{2} N_{p3} S}{3 \times J \times V_{DC}}$ |
| Secondary Voltage ($V_{s,rms}$) | $\frac{\pi\sqrt{2}}{4} \times V_{out}$ | $\frac{\pi\sqrt{2}}{6} \times V_{out}$ |
| Secondary current ($I_s$) | $\frac{2\sqrt{2} \times S}{\pi \times V_{out}}$ | $\frac{\sqrt{2} \times S}{\pi \times V_{out}}$ |
| Secondary area ($A_s$) | $\frac{2\sqrt{2} N_{s1} \times S}{\pi \times V_{out} \times J}$ | $\frac{\sqrt{2} N_{s3} \times S}{\pi \times V_{out} \times J}$ |
| Winding area ($A_w$) | $\frac{\sqrt{2} \times S}{J} \left[ \frac{N_{p1}}{V_{DC}} + \frac{2N_{s1}}{\pi V_{out}} \right]$ | $\frac{2\sqrt{2} \times S}{J} \left[ \frac{2N_{p3}}{3V_{DC}} + \frac{N_{s3}}{\pi V_{out}} \right]$ |
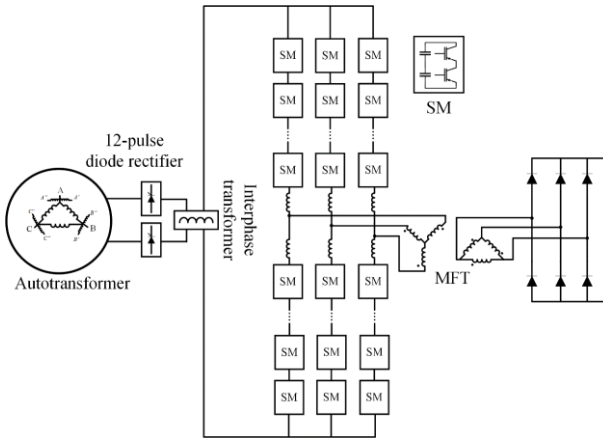
Fig. 3. Three-phase SST including the autotransformer, input rectifier, interphase transformer, MMC, MFT, and output rectifier

Although the area product of two cases are the same based on (9), three-phase MFT for this specific application (and similar applications connected to a medium-voltage grid deliver high current to the load) saves size and weight in comparison to a single-phase solution when the weight of the active part is considered. The three-phase transformer is smaller because the return path of the magnetic flux is completed through the legs of another phases. Therefore, the core can be selected smaller for the same power rating.

On the other hand, the power electronics section (MMC) must be designed three-phase or single-phase according to the structure of the SST. Authors of the present paper compared the single-phase and three-phase MMCs in [5] which focuses on the power electronics. The total rating of switching devices (number of switches × Rating voltage × Rating current) for single-phase and three-phase MMCs are the same; therefore, the total price of the switching devices are similar. Moreover, the three-phase MMC has better performance regarding the total harmonics distortion (THD). Then, it can be decided regarding the THD and MFT's weight and size. Therefore, the three-phase SST is more beneficial for green hydrogen production.

### III. Optimum Frequency Selection

Regarding the literature review in section II, the works which deal with higher power levels use lower frequencies because of several reasons (Fig. 4). Firstly, for a high-frequency SST, fast switching devices are needed; however, fast switching devices have lower voltage and current ratings. Secondly, higher frequency increases the losses in the MFT. On the one hand, no-load loss, which is mainly because of the
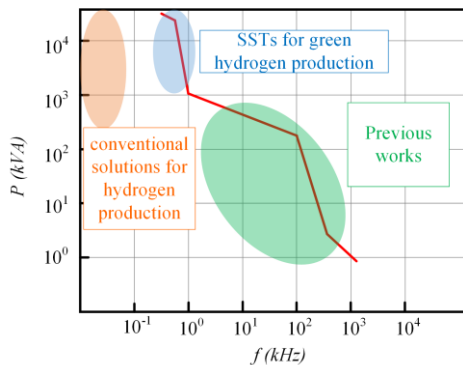
core loss, in the transformer depends on the frequency as follows [6]:

$$P_c = k \cdot f^\alpha \cdot B^\beta \qquad (10)$$

Where $k$, $\alpha$, and $\beta$ are Steinmetz coefficients and $B$ is the magnetic flux density. On the other hand, the higher frequency results in higher copper loss because of eddy currents in the conductors (skin effect and proximity effect). It is possible to mitigate the high-frequency losses by using ferrite, amorphous, and nanocrystalline materials for the transformer core and using litz wires for the windings. However, for large transformers, these materials and methods are not available. The only available core materials are electrical steel (SiFe) and amorphous. The windings are made of continuously-transposed conductors (CTC) to provide the necessary mechanical strength and overcome the copper loss. Another limitation of using higher frequency is thermal issues. The aim of higher frequency is to increase the power density of the SST. However, a smaller transformer has smaller heat transfer surfaces. Hence, the frequency of the SST cannot be selected above a certain level (a few hundred Hz). Fig. 5 compares the weight of active parts and the losses for various frequencies. Regarding Fig. 5, frequencies between 300 Hz and 400 Hz are reasonable for the green hydrogen production. For the frequencies less than 300 Hz the core loss is high and for frequencies more than 400 Hz the copper loss is problematic. Therefore, regarding the size of the active part, the frequency for the MFT in the present paper is selected at 400 Hz because the weight of active parts of 400 Hz transformer is 30% less than 300 Hz transformer.

### IV. Transformer Design

This section gives the transformer design for the green hydrogen production regarding the characteristic of Table III. As mentioned in Table III, the primary voltage of the transformer can be calculated as follows:

$$V_{Prms,L-L} = k_{au}k_rk_{MMC} \times V_{grid.rms,L-L} \qquad (11)$$

Where $k_{au}$ is the gain of the autotransformer, $k_r$ is the rectifier coefficient, $k_{MMC}$ is the MMC coefficient, and $V_{grid}$ is the voltage of the grid. Assuming $k_{au} = 1.0353$, $k_r = (3\sqrt{2})/\pi$, $k_{MMC} = \sqrt{6}/4$, and $V_{grid} = 33$ kV$_{rms,L-L}$ results in $V_{Prms,L-L} = 25.4$ kV. The core material is Metglas 2605SA1, hence, the maximum flux density can be selected 1.2 T. In order to minimize the ohmic loss, the number of turns must be selected as low as possible; however, the number of turns cannot be selected less than 2 turns because it is important to put all strands of the CTC in all positions. The minimum required length of the LV winding is obtained when $N_s = 2$. Thus, this value selected for number of turns in secondary. Since the configuration of the transformer is Yd, number of primary turns can be calculated as follows:
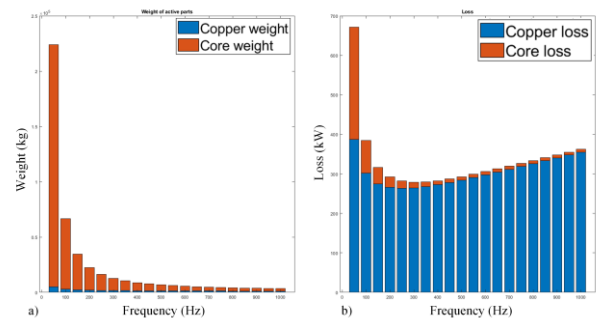


Fig. 4. The power rating vs frequency of the transformer in the green hydrogen production and reviewed works.



Fig. 5. Various frequencies comparison; a) weight of the active parts, b) losses

$$N_p = N_s \times \frac{V_p/\sqrt{3}}{V_s} = 52 \qquad (12)$$

The primary is made of 26 discs as shown in Fig. 6. The cross-section of primary and secondary are 240 mm$^2$ and 7410 mm$^2$, respectively. Note that secondary is made of 13 parallel paths, as shown in Fig. 7 (a). The winding begins from the bottom and turns are wound around the pressboard. Then a spacer is used to support the outer turn. The required core area can be calculated as follows:

$$A_c = \frac{V_{in}/\sqrt{3}}{k_c \times k_w \times B_m \times f \times N_p} \approx 1670 \; cm^2 \qquad (13)$$

Where $k_c$ is the core stack factor (=0.79) and $k_w$ is the waveform factor (=4.44). The conductors are configured as shown in Fig. 7. The mean length of primary and secondary turns is obtained as $MLT_p$ = 2.238 m and $MLT_s$ = 3.238 m, respectively. The losses are from a COMSOL simulation, at 75°C, as shown in Fig. 7. The core loss is 9.85 kW and the total copper loss is 272.47 kW. Accordingly, the total loss is 282.04 kW. The designed transformer is shown in Fig. 8. The weight of the active parts for the designed MFT is 8835 kg in comparison to a commercially available LFT which its weight of active parts is 29750 kg.

## V. CONCLUSION

In this paper using of SST for green hydrogen production is described. A comparative analysis of previous works and studies is presented. Single-phase and three-phase medium-frequency transformers are compared and shown that for applications which deliver huge current due to a step-down SST a three-phase configuration is more beneficial. Some evidence for selecting the optimum frequency are summarized and a brief design is presented to show that the weight of active parts of the designed MFT is 69% less than a similar trend in a conventional LFT.
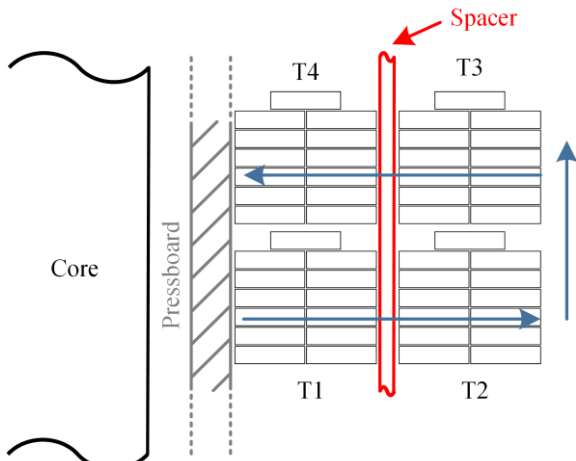


Fig. 6. The discs of the primary winding

TABLE III. THE CHARACTERISTICS OF THE DESIGNED TRANSFORMER

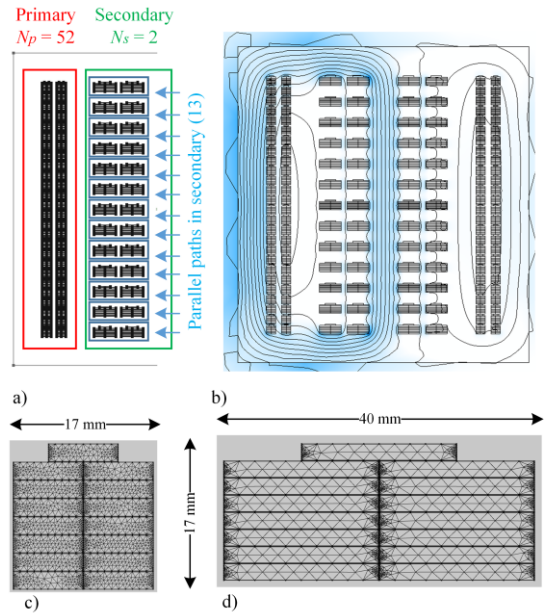| Parameter | Value | Unit |
|---|---|---|
| Rating Power | 25 | MVA |
| Frequency (f) | 400 | Hz |
| Primary voltage ($V_p$) | 25.4 | kV |
| Secondary voltage ($V_s$) | 560 | V |
| Primary current density ($J_p$) | 2.5 | A/mm |
| Secondary current density ($J_s$) | 2 | A/mm |
| Operation temperature | 75 | °C |



Fig. 7. COMSOL simulation; a) the geometry of the window, b) the plot of flux density (B), c) applied mesh on one primary conductor, d) applied mesh on one secondary conductor
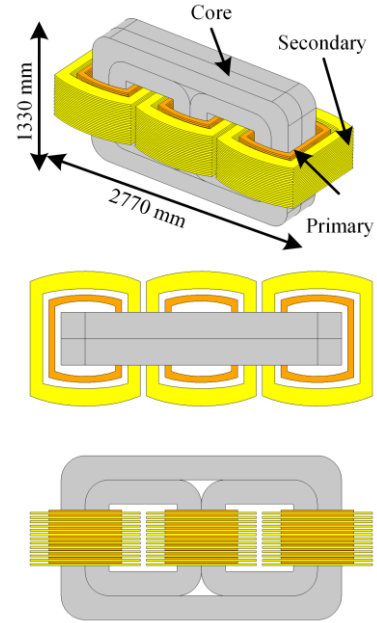


Fig. 8. The designed MFT

REFERENCES

[1] M. Kharezy, "A Novel Oil-immersed Medium Frequency Transformer for Offshore HVDC Wind Farms," PhD. Dissertation, Chalmers University of Technology, Gothenburg, Sweden, 2020.

[2] K. Sharifabadi, L. Harnefors, H. Nee, S. Norrga, R. Teodorescu, Design, Control, and Application of Modular Multilevel Converters for HVDC Transmission Systems, Wiley, 2016.

[3] R. J. G. Montoya, "High-Frequency Transformer Design for Solid-State Transformers in Electric Power Distribution Systems," MSc. Dissertation, University of Arkansas, Arkansas, the USA, 2015.

[4] C. W. T. McLyman, Transformer and Inductor Design Handbook, 4th ed., Boca Raton, FL, USA: CRC Press, 2011.

[5] Z. Li, Z. Qin, R. Mirzadarani, M. G. Niasar, P. Bauer, "Comparison of Modular Multilevel Converters based Solid State Transformer for ACDC Application," in TechRxiv (preprint).

[6] Hurley, W. G.; Wölfle Werner H, Transformers and Inductors for Power Electronics: Theory, Design and Applications, Hoboken: Wiley-Blackwell, 2013.

[7] L. Heinemann, "An actively cooled high power, high frequency transformer with high insulation capability," in *APEC. Seventeenth Annual IEEE Applied Power Electronics Conference and Exposition (Cat. No.02CH37335)*, Dallas, TX, USA, 2002.

[8] J. Taufiq, "Power Electronics Technologies for Railway Vehicles," in *Power Conversion Conference* , Nagoya, 2007.

[9] M. Pavlovsky, S. W. H. de Haan, J. A. Ferreira, "Design for better thermal management in high-power high-frequency transformers," in *Fourtieth IAS Annual Meeting. Conference Record of the 2005 Industry Applications Conference*, Hong Kong, China, 2005.

[10] M. Steiner and H. Reinold, "Medium frequency topology in railway applications," in *European Conference on Power Electronics and Applications*, Aalborg, 2007.

[11] T. Komrska and Z. Peroutka, "Main Traction Converter with Medium-Frequency Transformer: Control of Converters around MF Transformer," in *International Symposium on Power Electronics, Electrical Drives, Automation and Motion*, Ischia, Italy, 2008.

[12] S. Meier, T. Kjellqvist, S. Norrga and H. Nee, "Design considerations for medium-frequency power transformers in offshore wind farms," in *13th European Conference on Power Electronics and Applications*, Barcelona, Spain, 2009.

[13] T. Kjellqvist, S. Ostlund, S. Norrga and K. Ilves, "Thermal evaluation of a medium frequency transformer in a line side conversion system," in *13th European Conference on Power Electronics and Applications*, Barcelona, Spain, 2009.

[14] H. Hoffmann and B. Piepenbreier, "Medium frequency transformer for rail application using new materials," in *1st International Electric Drives Production Conference*, Nuremberg, Germany, 2011.

[15] I. Villar, L. Mir, I. Etxeberria-Otadui, J. Colmenero, X. Agirre and T. Nieva, "Optimal design and experimental validation of a Medium-Frequency 400kVA power transformer for railway traction applications," in *IEEE Energy Conversion Congress and Exposition (ECCE)*, Raleigh, NC, USA, 2012.

[16] A. Huang, X. She, X. Yu, F. Wang, and G. Wang, "Next generation power distribution system architecture: The future renewable electric energy delivery and management (FREEDM) system," *The Energy Internet. Proceedings of the,* vol. 99, no. 1, pp. 133-148, 2011.

[17] A. Huang, "Solid state transformer and FREEDM system power management strategies," in *NSF FREEDM Syst. Center NC State Univ*, Raleigh, NC, USA, 2016.

[18] G. Ortiz, "High-Power DC-DC Converter Technologies for Smart Grid and Traction Applications," PhD thesis. ETHZ, Zürich, 2014.

[19] "STS Transfo," 17 October 2022. [Online]. Available: https://sts-trafo.de/en/transformers.

[20] M. Jaritz and J. Biela, "Isolation design of a 14.4kV, 100kHz transformer with a high isolation voltage (115kV)," in *IEEE International Power Modulator and High Voltage Conference (IPMHVC)*, San Francisco, CA, USA, 2016.

[21] M. Mogorovic and D. Dujic, "Medium Frequency Transformer Design and Optimization," in *PCIM Europe 2017; International Exhibition and Conference for Power Electronics, Intelligent Motion, Renewable Energy and Energy Management*, Nuremberg, Germany, 2017.

[22] S. Zhao, Q. Li, F. C. Lee and B. Li, "High-Frequency Transformer Design for Modular Power Conversion From Medium-Voltage AC to 400 VDC," *in IEEE Transactions on Power Electronics,* vol. 33, no. 9, pp. 7545-7557, 2018.

[23] T. Hatakeyama, N. Kurita and M. Kimura, "Prototyping of 500 kVA Medium Frequency Transformer for Offshore Direct-Current Collection Grid," in *International Power Electronics Conference (IPEC-Niigata 2018 -ECCE Asia)*, Niigata, Japan, 2018.

[24] T. Guillod, R. Faerber, D. Rothmund, F. Krismer, C. M. Franck and J. W. Kolar, "Dielectric Losses in Dry-Type Insulation of Medium-Voltage Power Electronic Converters," *IEEE Journal of Emerging and Selected Topics in Power Electronics,* vol. 8, no. 3, pp. 2716-2732, 2020.

[25] A. El Shafei, S. Ozdemir, N. Altin, G. Jean-Pierre and A. Nasiri, "Development of a Medium Voltage, High Power, High Frequency Four-Port Solid State Transformer," *CES Transactions on Electrical Machines and Systems,* vol. 6, no. 1, pp. 95-104, 2022.

[26] Z. Guo, R. Yu, W. Xu, X. Feng and A. Q. Huang, "Design and Optimization of a 200-kW Medium-Frequency Transformer for Medium-Voltage SiC PV Inverters," *IEEE Transactions on Power Electronics,* vol. 36, no. 9, pp. 10548-10560, 2021.

[27] Z. Yi, K. Sun, H. Liu, G. Cao and S. Lu, "Design and Optimization of the Insulation of Medium-voltage Medium-frequency Transformers for Solid-state Transformers," *IEEE Journal of Emerging and Selected Topics in Power Electronics,* vol. 10, no. 4, pp. 3561-3570, 2022.

[28] G. Wang, S. Baek, J. Elliott, A. Kadavelugu, F. Wang, X. She, S. Dutta, Y. Liu, T. Zhao, W. Yao, R. Gould, S. Bhattacharya, A. Huang, "Design and hardware implementation of Gen-1 silicon based solid state transformer," in *Twenty-Sixth Annual IEEE Applied Power Electronics Conference and Exposition (APEC)*, Fort Worth, TX, USA, 2011.

[29] C. Zhao, D. Dujic, A. Mester, J. Steinke, M. Weiss, S. Lewdeni, T. Chaudhuri, P. Stefanutti, "Power Electronic Traction Transformer—Medium Voltage Prototype," *IEEE Transactions on Industrial Electronics,* vol. 61, no. 7, pp. 3257-3268, 2014.

[30] M. A. Bahmani, "Design and Optimization Considerations of Medium-Frequency Power Transformers in High-Power DC-DC Applications," PhD. Dissertation, Chalmers University of Technology, Gothenburg, Sweden, 2016.

[31] N. Kimura, T. Morizane, I. Iyoda, K. Nakao, T. Yokoyama, "Solid state transformer investigation for HVDC transmission from offshore windfarm," in *IEEE 6th International Conference on Renewable Energy Research and Applications (ICRERA)*, San Diego, CA, USA, 2017.

[32] T. Gradinger, U. Drofenik, and S. Alvarez, "Novel Insulation Concept for an MV Dry-Cast Medium-Frequency Transformer," in *Proceedings of the 19th European Conference on Power Electronics and Applications (EPE 2017 - ECCE Europe)*, Warsaw, Poland, 2017.

[33] W. Wang, Y. Liu, J. He, D. Ma, L. Hu, S. Yu, S. Li, J. Liu, "An Improved Design Procedure for A 10 kHz, 10 kW Medium-Frequency Transformer Considering Insulation Breakdown Strength and Structure Optimization," *in IEEE Journal of Emerging and Selected Topics in Power Electronics,* vol. 10, no. 4, pp. 3525-3540, 2022.

[34] Hugo, N., Stefanutti, P., Pellerin, M., "Power electronics traction transformer," in *European Conference on Power Electronics and Applications*, Aalborg, 2007.